DOI: 10.61782/fa.2025.0446

IMPACT OF ACOUSTIC TEST FIXTURE EAR STIFFNESS ON EARPLUG ATTENUATION OF IMPULSIVE SOUNDS.

Christophe Ruzyla[1,2*] **Cyril Blondé-Weinmann**[1] **Pascal Hamery**[1] **Franck Sgard**[3] **Sébastien Roth**[2]

[1] Department Acoustics and Soldier Protection, French-German Research Institute of Saint-Louis, 68300 Saint-Louis, France

[2] Laboratoire Interdisciplinaire Carnot de Bourgogne, site UTBM, UMR 6303 CNRS / Université de Technologie de Belfort-Montbéliard, France.

[3] Institut de Recherche Robert-Sauvé en Santé et Sécurité du Travail, Montréal (QC), Canada.

ABSTRACT

Acoustic Test Fixtures (ATFs) are physical substitutes designed to evaluate the attenuation provided by Hearing Protection Devices (HPD). These devices are particularly useful for measurements, where human testing is not feasible, such as high-level impulse noises exposure. However, challenges arise in integrating the mechanical elements required to mimic the response of the human head. The material properties of commercially available ATFs vary, potentially leading to different coupling with HPDs. This study aims to investigate the behavior of a rigid earplug and the resulting acoustic pressure in the ear canal when the stiffness of the ATF ear is modified. An experimental setup was developed, involving a custom laboratory-developed ATF to estimate a rigid earplug attenuation for three simplified ear materials of increasing stiffness. Additionally, a time-domain numerical model using finite element method was created to study the wave propagation in the simplified ATF ear. This study shows experimentally and numerically that the stiffness of the ATF ear significantly influences earplug attenuation measurements by modifying the contribution of tissular conduction in the wave propagation behind the protector. This study paves the way for improving ATF biofidelity by more accurately accounting for the behavior of the human outer ear mechanical properties.

*Corresponding author: christophe.ruzyla@isl.eu.

Keywords: *Hearing protection, acoustic test fixture, impulsive noise, finite element method.*

1. INTRODUCTION

Impulse noises are characterized by a high amplitude, a sudden onset, and a brief duration [1]. These noises can be encountered on the battlefield, where soldiers are exposed to impulsive noise levels ranging from 145 dB-peak to 190 dB-peak [1-2]. To ensure adequate protection, it is necessary to accurately assess the performance of Hearing Protection Devices (HPD). Acoustic Test Fixtures (ATF) are commonly used to estimate the attenuation allowed by HPD facing very high-level impulse noises. Nevertheless, the ATF correspond only to an approximation of the human auditory system, whether it concerns the eardrum, the Ear Canal (EC) anatomy, or the material properties [3]. More specifically, the interactions between the very high-level impulse wave and the HPD, as well as the transmission paths through the outer ear's tissues and the HPD, still need to be fully assessed for the current ATF. These transmissions strongly depend on the materials used in the ATF [4], but a clear relationship is not yet fully understood and requires further investigation.

This paper aims to investigate the relation between artificial ear material properties and earplug sound attenuation. An experimental setup was developed, involving a custom laboratory-developed ATF to estimate a rigid earplug attenuation for three geometrically simplified ear materials of increasing stiffness. Additionally, a time-domain numerical model using finite element method was created to study the wave propagation in the simplified ATF ear.

2. EXPERIMENTAL STUDY

2.1 Material and method

The laboratory-designed ATF used in this study, shown in Figure 1, is a modification of the ISL standard ATF that complies with the S.12.42 standard [5]. This laboratory-developed artificial head incorporates the electronics and measuring devices of the standard ISL head. It is modified to allow the installation of an ear flange (diameter 100 mm, thickness 8.5 mm) made from a single homogeneous material. This ear is held in position on the artificial head by an aluminum ring secured by 6 screws.

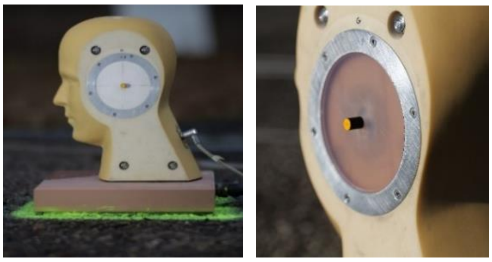

Figure 1 : View of the custom-made ATF (left) and a close-up of the ear flange (right).

For this study, three different ear materials of variable stiffness were considered. Their mechanical properties were measured through a compression test compliant with ASTM D575 and are shown in Table 1. The RTV 3325 ear was produced by molding. The other two ears were fabricated using 3D printing (Formlabs Form 3L).

Table 1. Average mechanical properties of the ears tested in the study with standard deviations.

Name	Young modulus [MPa]	Density [g/m^3]	Poisson's ratio [-]
RTV 3325	0.71 ± 0.02	1.21 ± 0.01	0.38 ± 0.03
Formlabs 50A	4.76 ± 0.16	1.09 ± 0.01	0.47 ± 0.01
Formlabs Draft	(1.40 ± 0.06) $\times 10^3$	1.19 ± 0.01	0.47 ± 0.01

The measurements were conducted in an anechoic chamber. The source of impulsive noise was a laboratory shock tube [6] placed 4 meters from the ATF. A reference microphone was positioned at equidistance from the source to measure the external pressure (Brüel & Kjær ½"). The pressure in the EC was recorded by an ear simulator compliant with IEC 60318-3 standard. In this configuration, the head was subjected in a reproducible manner to an impulse noise of 136 ± 1 dB-peak.

The tests presented in this paper were carried out at normal incidence to the ear. The earplugs used are 3D printed with a cylindrical shape (diameter: 8 mm, length 20 mm) and are made of Acrylonitrile Butadiene Styrene (ABS). They were inserted 10 mm into the ears. The external pressure and the pressure under the earplug were recorded simultaneously with a TEAC LX10 data recorder. Measurements on each ear were conducted five times, to verify the repeatability.

2.2 Results

The average acoustic pressure history measured inside the occluded EC is shown in Figure 2.

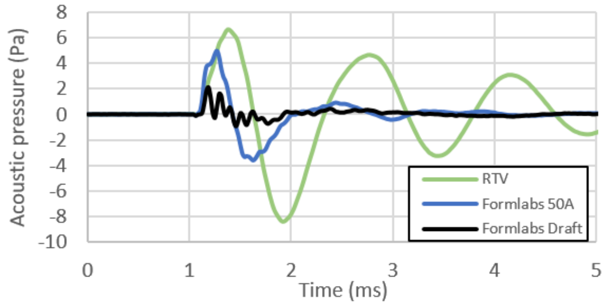

Figure 2. Average acoustic pressure measured inside the occluded EC.

Noise reduction (NR), i.e., the difference in peak levels between the pressure in front of the ear and the pressure in the occluded EC, has been determined for each configuration and is presented in Table 2.

Table 2. NR for the three ear materials tested.

Name	NR peak [dB]
RTV 3325	23.6
Formlabs 50A	28.7
Formlabs Draft	36.3

As shown in Table 2, peak noise reduction decreases with increasing rigidity of the ear flange. The three ears Insertion Losses (IL) were determined for the previously described impulse stimulation. From 100 to 400 Hz, an increase in IL of 12.9 dB per octave and 13.6 dB per octave was observed for the Formlabs 50A and Draft ears, respectively. From 200 Hz to 1 kHz, insertion loss was higher with increasing rigidity. In particular, at 700 Hz, we observe the largest deviations in IL. At this frequency, the IL was 17 dB, 30 dB, and 42 dB for the ear made of RTV, Formlabs 50A, and Draft, respectively. After 1 kHz, there are no marked differences between the different flanges.

3. NUMERICAL MODEL

To complete the experimental study, a numerical model of the laboratory-developed artificial head described in section 2.1 was developed. It allows for a more comprehensive analysis by estimating, in addition, the displacements of the protector and ear canal walls or the effect of potential micro-leaks. This time-domain finite element model is solved using COMSOL Multiphysics® (Stockholm, Sweden).

3.1 Methods

The 2D-axisymmetric numerical model developed comply with the ear flange geometry and is composed of four domains, represented in Figure 3. The earplug (labelled 2 in Fig. 3) and ear flange are considered as elastic solid materials, while the external air domain and the air in the EC (labelled 3 in Fig. 3) are modeled as fluid domains, satisfying the lossless Helmholtz equation. The mechanical properties applied to the three ear flanges correspond to the data determined experimentally in Table 1. The air fluid is defined by a density of 1.2 kg/m^3 and a sound speed of 343 m/s at 20°C. The earplug is made of ABS with a Young's modulus of 2200 MPa, a Poisson's ratio of 0.35 and a density of 1040 kg/m^3 [6]. No damping is applied in the solid domains.
The averaged incident sound pressure measured experimentally is used as input to a plane wave radiation condition applied at the bottom of the inlet air domain. The lateral sides of the ear flange are fixed boundary conditions (black lines in Fig.3) and constrained displacement conditions (green lines in Fig.3). These conditions were chosen based on practical insights into the integration of the ear flange with the ATF. An ear simulator consists of a main cavity and two slits to simulate the impedance of the middle ear. To evaluate the acoustic pressure at the ATF microphone position, the main cavity of the coupler has been represented along its entire length. The equivalent impedance of the two slits has been applied by a frequency-dependent impedance condition [7] at the ATF microphone position (purple line in Fig. 3). A fluid-structural coupling exists between EC and ear flange (yellow line labelled 1 in Fig. 3).
The equations in the air and solid domains are solved using at least five quadratic elements per wavelength (maximal resolution frequency was set to 10 kHz) ensuring solution convergence. The time-stepping method generalized-alpha is used to solve the problem. Both acoustic pressure in the EC and inlet air domain, as well as earplug and ear structural displacement fields are computed.

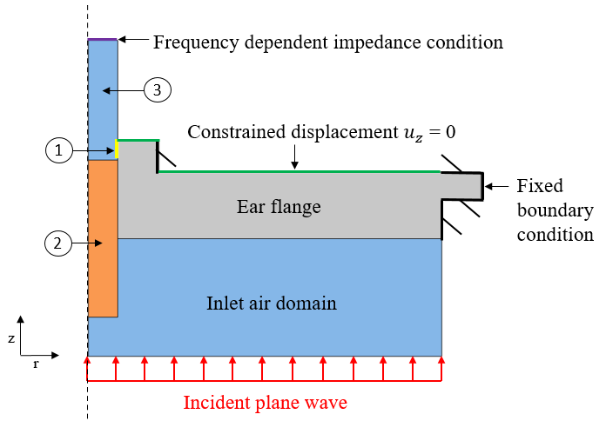

Figure 3. Geometry and boundary conditions of the FE model. The symmetry axis is shown as a dotted line. (1) interface between EC air domain and the ear flange, (2) earplug, (3) EC air domain.

3.2 Results

Figure 4 shows the comparison between experimentally and numerically evaluated acoustic pressure time history in the occluded EC for the RTV ear. The numerical model yields a good pressure estimate, but exhibits undamped oscillations and combined contribution effects. Comparisons of the numerical simulations with the experimental results for the Formlabs 50A and Draft ear (not shown here for the sake of conciseness) indicate notably the presence of leakage during the experiment.
The displacement time history of the earplug (labelled 2 in Fig. 3) in longitudinal direction and of the EC air domain/ear flange interface (boundary 1 in Fig. 3) in radial direction are also represented. These undamped oscillating displacements present a first peak amplitude of 0.60 µm and 0.25 µm for the earplug and the ear canal/ear flange interface, respectively.

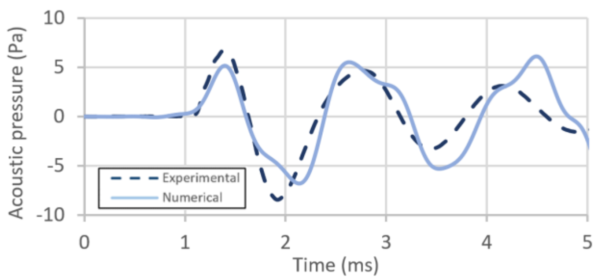

(a) Average acoustic pressure in the EC, (3) in Fig.3

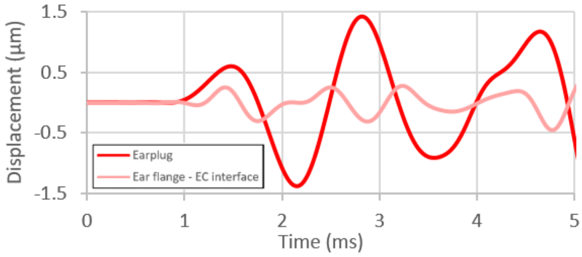

(b) Simulated surface-average displacement of the earplug's domain (in z-direction), (1) in Fig.3, and of ear flange EC/interface (in r-direction), (2) in Fig.3.

Figure 4. Average acoustic pressure and displacements for the artificial ear in RTV.

4. DISCUSSION

The mechanical properties of the artificial ear significantly influence the attenuation provided by earplugs. Specifically, the peak noise reduction is enhanced as the stiffness of the outer ear increases. A previous experimental study has demonstrated the impact of outer ear hardness on the earplug "piston effect" [4]. This effect is characterized by a resonant, back-and-forth rigid body motion of the earplug coupled with the external auditory canal wall, typically occurring at frequencies below 2 kHz. The piston effect may account for some of the discrepancies observed at low-frequency for the earplug insertion loss among the three tested ears.

Analytically, the contribution of the piston effect to variations in ear canal sound pressure can be estimated by considering the relative equivalent occluded ear canal volume change and the adiabatic bulk modulus of air. Estimations based on numerically determined displacements reveal that for the softer ear made with RTV, 63% of the first peak acoustic pressure is attributable to the piston effect and 37% to the ear canal wall vibrations. For higher hardness (displacements curves omitted in this article), this second contribution rises to 38% for the Formlabs 50A ear and 44% for the Draft ear. Thus, the earplug piston effect contribution is predominant for the three ears tested but decreases with the ear's stiffness. The relative importance of these contributions to the human ear remains to be clarified.

Besides, stiffer materials induce additional effects. A low IL can be observed at lower frequencies, especially for the Formlabs 50A and the Formlabs Draft, indicating leakage during experimental measurements. These leakages can be attributed to improper seals between earplugs and EC walls due to the surface's conditions. Indeed, slight grooves could be seen on the earplug (3D printed) and EC surfaces.

5. CONCLUSION

Experimental measurements have quantified the impact of a modification in the stiffness of the ear on the attenuation of a protector. Specifically, peak noise reduction increases with ear stiffness. For the various ear materials, the protector and the EC wall displacements have been estimated numerically and discussed. This study shows that the earplug displacement is the main contribution to the pressure in the EC. The vibration of the interface EC / ear flange has a non-negligible effect, with a contribution increasing with ear stiffness. Finally, these results pave the way for improving ATFs by better reproducing the behavior of earplugs in human ears.

6. REFERENCES

[1] D. Smeatham and P. D. Wheeler, "On the Performance of Hearing Protectors in Impulsive Noise," *Appl. Acoust.*, vol. 54, no. 2, pp. 165-181, 1998.

[2] L. Humes, L. M. Joellenbeck and J. S. Durch, "Noise and Military Service : Implications for Hearing Loss and Tinnitus.," The National Academies Press, 2006.

[3] E. H. Berger, "Preferred Methods for Measuring Hearing Protector Attenuation,," *INTER-NOISE conference*, 2005.

[4] C. Blondé-Weinmann, P. Hamery, V. Zimpfer and S. De Mezzo, "Effects of the earplug and external ear hardness of the direct transmissions induced by high-level impulse noises," in *INTER-NOISE conference*, Nantes, 2024.

[5] P. Hamery, V. Zimpfer, K. Buck and S. De Mezzo, "Very high level impulse noises and hearing protection," in *Euronoise conference*, Maastricht, 2015.

[6] C. Blondé-Weinmann, "Description et caractérisation des phénomènes impliqués dans la limitation des protections auditives lors d'impulsions de fort niveau.," *Ph.D. thesis*, 2023.

[7] H. Wang and M. Hornikx, "Time-domain impedance boundary condition modeling with the discontinuous Galerkin method for room acoustics simulations," *J. Acoust. Soc. Am.*, vol. 147, no. 4, p. 2534–2546, 2020.